A theoretical analysis of an optimal chainring shape to maximize crank power during isokinetic pedaling

Jeffery W. Rankin, Richard R. Neptune*

Department of Mechanical Engineering, The University of Texas at Austin, 1 University Station C2200 Austin, TX 78712, USA

Abstract

Previous studies have sought to improve cycling performance by altering various aspects of the pedaling motion using novel crank–pedal mechanisms and non-circular chainrings. However, most designs have been based on empirical data and very few have provided significant improvements in cycling performance. The purpose of this study was to use a theoretical framework that included a detailed musculoskeletal model driven by individual muscle actuators, forward dynamic simulations and design optimization to determine if cycling performance (i.e., maximal power output) could be improved by optimizing the chainring shape to maximize average crank power during isokinetic pedaling conditions. The optimization identified a consistent non-circular chainring shape at pedaling rates of 60, 90 and 120 rpm with an average eccentricity of 1.29 that increased crank power by an average of 2.9% compared to a conventional circular chainring. The increase in average crank power was the result of the optimal chainrings slowing down the crank velocity during the downstroke (power phase) to allow muscles to generate power longer and produce more external work. The data also showed that chainrings with higher eccentricity increased negative muscle work following the power phase due to muscle activation–deactivation dynamics. Thus, the chainring shape that maximized average crank power balanced these competing demands by providing enough eccentricity to increase the external work generated by muscles during the power phase while minimizing negative work during the subsequent recovery phase.

1. Introduction

A considerable number of pedaling studies have sought to improve cycling performance by changing various aspects of the pedaling motion through novel crank–pedal mechanisms and non-circular chainring shapes (e.g., Hue et al., 2001; Lucia et al., 2004; Santalla et al., 2002; Zamparo et al., 2002). A conventional circular chainring provides a constant radius from the crank center to the chain driving the rear wheel, which provides a relatively constant crank angular velocity profile. In contrast, the radius of a non-circular chainring varies as a function of crank angle, and therefore alters the crank angular velocity profile over the pedaling cycle. The modified velocity profile alters the leg kinematics throughout the pedaling

motion, and therefore has the potential to alter the contractile state of muscles (i.e., fiber length and velocity) and provide improved conditions for generating muscle power.

Previous studies analyzing non-circular chainrings have sought to improve performance by either increasing maximum power output or improving efficiency by reducing the metabolic cost ($\dot{V}O_2$) required to generate a given level of crank power. Martin et al. (2002) showed an increase in maximum instantaneous power for single-leg cycling while using an offset chainring that allowed more time to be spent during the downstroke, but did not investigate normal bilateral pedaling. Okajima (1983) concluded that the non-circular Biopace chainring (Shimano, Inc.), which is similar in shape to an ellipse but with non-perpendicular major and minor axes, improved cycling efficiency by reducing leg joint torques and muscle EMG relative to those of a circular chainring at a given power

*Corresponding author. Tel.: +1 512 471 0848; fax: +1 512 471 8727.
E-mail address: rneptune@mail.utexas.edu (R.R. Neptune).

output. However, subsequent studies showed no significant difference in $\dot{V}O_2$ consumption or heart rate in competitive cyclists when using Biopace versus circular chainrings (Cullen et al., 1992; Hull et al., 1992). Ratel et al. (2004) found that the Harmonic chainring (Somovedi S.A.M., Monaco), best described as two tangential curves with symmetry about a central point of rotation, did not significantly increase power output during maximal tests or reduce $\dot{V}O_2$ uptake and heart rate during tests at submaximal work rates in trained cyclists. The lack of significant improvements in cycling performance in the majority of these studies may be due to their development being based on empirical methods rather than on theoretical analysis.

Kautz and Hull (1995) was one of the few theoretical studies that sought to design a non-circular chainring to improve cycling performance by utilizing a torque-driven musculoskeletal model and dynamic optimization to determine the optimal chainring shape that minimized joint torques while pedaling at 90 rpm and 250 W. While the study successfully produced a chainring shape that reduced the net joint torques relative to a circular chainring, the optimized shape required peak forces to be generated in a region of the crank cycle when the joint angular velocities were highest. As they noted, this is not optimal in light of intrinsic muscle properties, specifically the force–velocity relationship. Thus, their optimal design would most likely change if muscle mechanics were included in their model. In addition, Kautz and Hull (1995) did not investigate the influence that pedaling rate may have on the optimal shape. Although most cyclists prefer pedaling near the 90 rpm rate (e.g., Hagberg et al., 1981; Marsh and Martin, 1993), Neptune and Kautz (2001) showed that muscle activation and deactivation dynamics can potentially influence muscle work production during fast cyclical movements such as those encountered during pedaling, suggesting that the optimal chainring shape may vary with pedaling rate.

The purpose of the study was to build upon the work of Kautz and Hull (1995) by developing a musculoskeletal model and simulation of pedaling driven by individual muscle actuators governed by intrinsic muscle properties (i.e., the force–length–velocity relationships) and using a dynamic optimization framework to identify the chainring shape that maximizes average crank power during iso-kinetic pedaling. While the focus of this study was on optimizing the chainring shape at the preferred pedaling rate of 90 rpm, the optimization framework was also used to determine if the optimal chainring shape varies with pedaling rate.

2. Methods

2.1. Overview

A detailed musculoskeletal model, forward dynamic simulation and dynamic optimization were used to determine the muscle excitation

pattern and chainring shape that maximized average crank power over the pedaling cycle at pedaling rates of 60, 90 and 120 rpm. In order to provide a basis for comparison with the optimal non-circular chainring, a second optimization was performed at each pedaling rate using a conventional circular chainring in which only muscle excitation patterns were optimized. The musculoskeletal model and optimization framework used in the analyses are described in detail below.

2.2. Musculoskeletal model

The model was developed using SIMM (Musculographics, Inc.) and consisted of nine segments including a pelvis, two legs, and a crank and pedal system (Fig. 1). Each leg consisted of thigh, shank, patella and foot segments. The pelvis and crank segments were fixed to ground and the crank segment was allowed to rotate about its midpoint. Standard 175 mm crank arm lengths were used and the foot segment was fixed to the pedal to represent standard pedals with clips. All joints were modeled as revolute joints except those of the knee and patella, which were prescribed to follow a planar motion specified as a function of knee flexion angle (Yamaguchi and Zajac, 1989). Passive torques representing the forces applied by ligaments, passive tissue and joint structures were applied at the hip, knee and ankle joints (Davy and Audu, 1987). The resulting model had three rotational degrees of freedom (the crank and two pedal angles). However, the motion of the crank was prescribed in order to emulate an isokinetic ergometer with crank kinematics defined by the chainring shape. The resulting dynamical equations of motion were then generated using SD/FAST (Parametric Technology Corp.) and a forward dynamic simulation was produced using Dynamics Pipeline (Musculographics, Inc.).

The major lower-extremity muscles of each leg were represented by 15 musculotendon actuators that were combined into 10 muscle groups based on anatomical classification (Fig. 1). A Hill-type muscle model was used that incorporated both passive and active muscle force generation and was governed by the force–length–velocity intrinsic muscle relationships (Zajac, 1989). Activation–deactivation dynamics were modeled with a first order differential equation that coupled muscle activation to the neural excitation pattern (Raasch et al., 1997). The activation and deactivation time constants for the differential equation were set to 10 and 20 ms, respectively, for each muscle actuator. The excitation patterns for the two legs were considered symmetric and 180° out of phase.
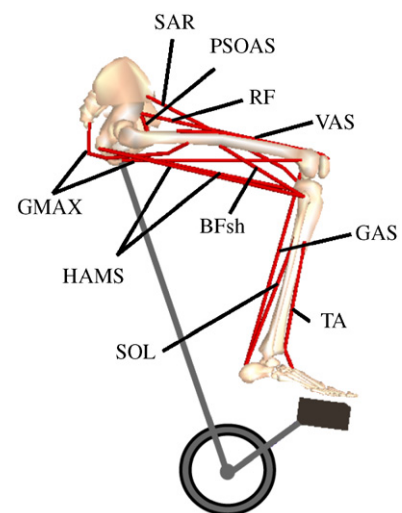

Fig. 1. Right leg of the bipedal bicycle-rider musculoskeletal model. The 10 muscle groups included in the model are SAR (sartorius), PSOAS (iliacus, psoas), RF (rectus femoris), VAS (three component vastus), TA (tibialis anterior), SOL (soleus), GAS (gastrocnemius), BFsh (biceps femoris short head), HAMS (medial hamstrings, biceps femoris long head), and GMAX (gluteus maximus, adductor magnus).

2.3. Dynamic optimization

A simulated annealing algorithm (Goffe et al., 1994) was used to perform several dynamic optimizations. In each optimization, the optimal excitation and chainring parameters that maximized average crank power over a full crank revolution were simultaneously determined (described below).

2.3.1. Muscle excitation patterns

The neural excitation for each muscle group was represented by a parameterized Gaussian pattern, given by the equation

$$u(t) = A\mathrm{e}^{-0.5|((t-\mu)/\sigma)^n|} \tag{1}$$

where $u(t)$ is the excitation value at time t; A the scaling factor (range 0–1, with 1 indicating full excitation); μ the center point of the excitation; σ the duration of the excitation; and n the shape factor.

This parameterization allowed excitation patterns ranging from single block to smooth Gaussian patterns with unconstrained timing. The optimization framework identified the four parameters (A, μ, σ, n) associated with each muscle group (40 parameters total) that maximized average crank power.

2.3.2. Chainring shape

To optimize the chainring, the shape was first parameterized as a function of crank angle (θ) using four variables defined as follows:

$$\begin{aligned} X(\theta) &= A(\cos(\theta))^{n_1} \\ Y(\theta) &= B(\sin(\theta))^{n_2} \end{aligned} \tag{2}$$

where $X(\theta)$ is the distance from the center of the chainring to the edge in the horizontal (x) direction (mm); $Y(\theta)$ the distance from the center of the chainring to the edge in the vertical (y) direction (mm); A, B the scaling factors in the x and y directions (mm), respectively; n_1, n_2 the shape factors.

This formulation allowed for a wide range of shapes including circles, ovals, skewed ellipses and smooth squares. A fifth chainring parameter (φ) was then used to rotate the chainring relative to the vertical axis to identify the optimal chainring orientation.

The shape was constrained such that (1) the circumference remained the same as a 42-tooth chainring, (2) the chainring path was continuous, and (3) the shape was void of concave regions. The instantaneous chainring angular velocity was then calculated as a function of crank angle as

$$V_{\mathrm{nc}}(\theta) = V_{\mathrm{c}}\left(\frac{r_{\mathrm{c}}}{r_{\mathrm{nc}}}\right) \tag{3}$$

where V_{nc} is the instantaneous angular velocity of the non-circular chainring at crank angle θ; V_{c} the angular velocity of the circular chainring (a constant based on the pedaling rate constraint); r_{c} the radius of a 42-tooth circular chainring; r_{nc} the instantaneous radius of the non-circular chainring at each θ.

The instantaneous angular velocity was then used to prescribe the crank velocity over the entire cycle emulating an isokinetic ergometer.

2.4. Analysis

A simulation of four consecutive crank cycles was generated and the data were analyzed during the fourth revolution to allow initial transient effects to dampen out and assure the simulation had reached steady-state. Following each optimization, the performance of the optimal chainring relative to the circular chainring was determined by comparing the average crank power during the final revolution. Individual muscle mechanical work was then determined by time integrating the musculotendon power within four regions of the crank cycle (Fig. 2) to gain insight into the source of any changes in crank power between the optimal and circular chainring shapes.
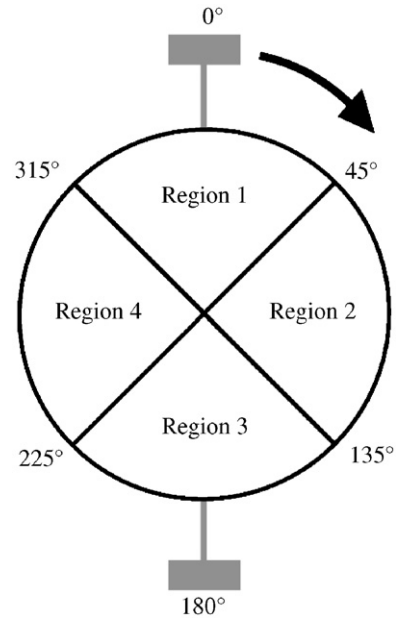

Fig. 2. The four regions of the crank cycle used to evaluate changes in muscle work between the optimal and circular chainrings. Crank angle is defined as 0° when the crank arm is at top-dead-center as shown.

3. Results

The optimization successfully identified an elliptical chainring with an eccentricity (i.e., the ratio of major to minor axes lengths) of 1.29, which increased the average crank power by 3.0% at 90 rpm (Table 1). The major axis (corresponding to the center point of the slowest crank angular velocity; Fig. 3) was rotated counterclockwise 91.8° relative to the crank arm (Fig. 4). The increase in average crank power was due primarily to increased muscle mechanical work from VAS, GMAX, SOL and GAS in Region 2 and PSOAS and TA in Region 4 (Fig. 5). In contrast, the net muscle work generated in Regions 1 and 3 (the transition regions) decreased.

The optimizations at the lower and higher pedaling rates produced chainrings of similar shape to that obtained at 90 rpm, with eccentricities of 1.35 and 1.24 and major axis orientations counterclockwise from the crank arm of 84.9° and 91.9° for the 60 and 120 rpm rates, respectively (Table 1, Fig. 4). The average crank power also increased relative to the circular chainring by 2.9% (Table 1). Muscle excitation timing of the various muscle groups for all pedaling rates occurred primarily when the muscles were shortening to maximize the power output (e.g., Fig. 6). Pedal kinematics for all chainrings were within two standard deviations of previously collected experimental measures at the same pedaling rate (data from Neptune and Herzog, 1999).

4. Discussion

The primary objective of this study was to determine if a non-circular chainring exists that improves cycling

Table 1
Average crank power for the conventional circular chainring and corresponding percent increase and eccentricity for the optimal chainring shape at the three pedaling rates

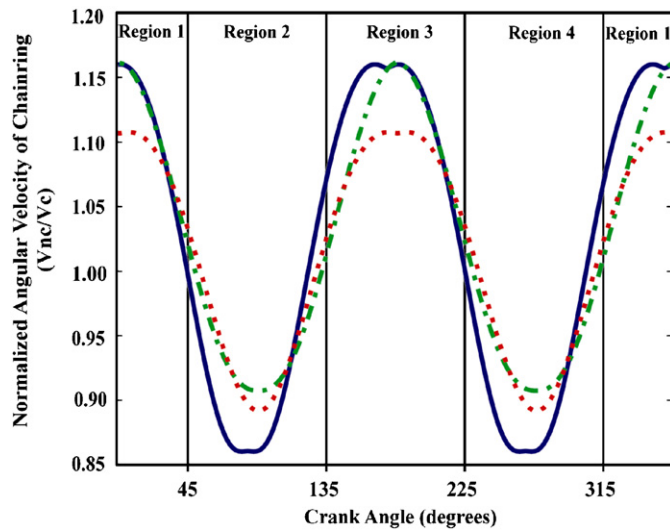| Pedaling rate (rpm)	Circular chainring Average power (W)	Optimal chainring Average power (W)	% Increase in power	Eccentricity
60	834.6	858.4	2.9	1.35
90	997.4	1027.4	3.0	1.29
120	1022.8	1052.8	2.9	1.24

Fig. 3. Optimal chainring velocity (V_{nc}) profiles normalized to the constant velocity of a circular chainring (V_c) over a single-pedaling cycle. The solid, dash-dot and dotted lines represent the optimal chainring velocities at 60, 90 and 120 rpm, respectively. Crank angle is defined as $0°$ at top-dead-center and positive in the clockwise direction.
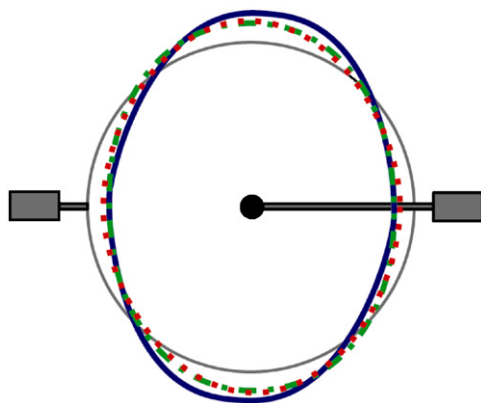

Fig. 4. Optimal chainring shapes for each pedaling rate. The solid, dash-dot and dotted lines represent the optimal chainring shapes at 60, 90 and 120 rpm, respectively. The thin line corresponds to a circular 42-tooth chainring. The crank arm and pedals are shown in reference to the optimal orientation.

performance by increasing maximal power output relative to a conventional circular chainring during isokinetic pedaling. At 90 rpm, a chainring shape was found that produced 3.0% more power than the corresponding circular chainring, which was consistent with a recent study analyzing a chainring of similar shape and eccentricity that enabled cyclists to produce 3% more power during an incremental workload test near 90 rpm (Martinez et al., 2006). Both the shape and orientation of the optimal chainring were different than that found by Kautz and Hull (1995) for endurance cycling, whose chainring had an orientation approximately 60° out-of-phase and 36% greater eccentricity. The present study also found the optimal chainring shapes while pedaling at 60 and 120 rpm were similar in shape to that at 90 rpm and improved power output by 2.9% (Table 1, Fig. 4). Throughout all the optimizations, we found the solutions to be very robust, with the algorithm producing similar chainring shapes regardless of the initial starting parameters.

We expected any crank power increase to be a direct result of the optimal chainring taking advantage of intrinsic muscle properties such as the force–length–velocity relationships, as these are important properties that affect maximal muscle power output (e.g., Durfee and Palmer, 1994; Huijing, 1998). For example, previous studies have shown that peak muscle power occurs at approximately one-third the maximum contraction velocity (e.g., Sargeant, 1994). Thus, we expected the optimal chainring shape to take advantage of the force–velocity relationship by allowing the primary power producing muscles (e.g., hip and knee extensors) to operate near the optimal velocity in order to produce more power. However, this was not the case. Examination of the fiber lengths and velocities during their active state showed that they were nearly identical between the optimal and circular chainrings at all pedaling rates (e.g., Fig. 7).

The increase in crank power was the result of the optimal chainring shape acting to slow down the crank angular velocity during the power phase (Fig. 3, Region 2), which allowed muscles to generate power longer and produce more external work. The hip and knee extensors (VAS, GMAX) and the ankle plantar flexors (SOL, GAS) all produced increased muscle work during the power phase (Fig. 5, Region 2) while, in the upstroke there was a small increase in hip flexor (PSOAS) and ankle dorsiflexor (TA) work (Fig. 5, Region 4, corresponding contralateral leg power phase). These results were consistent with a number of previous pedaling studies. Martin et al. (2002) showed maximal crank power can be increased 4% by offsetting a conventional chainring to allow more time in the power
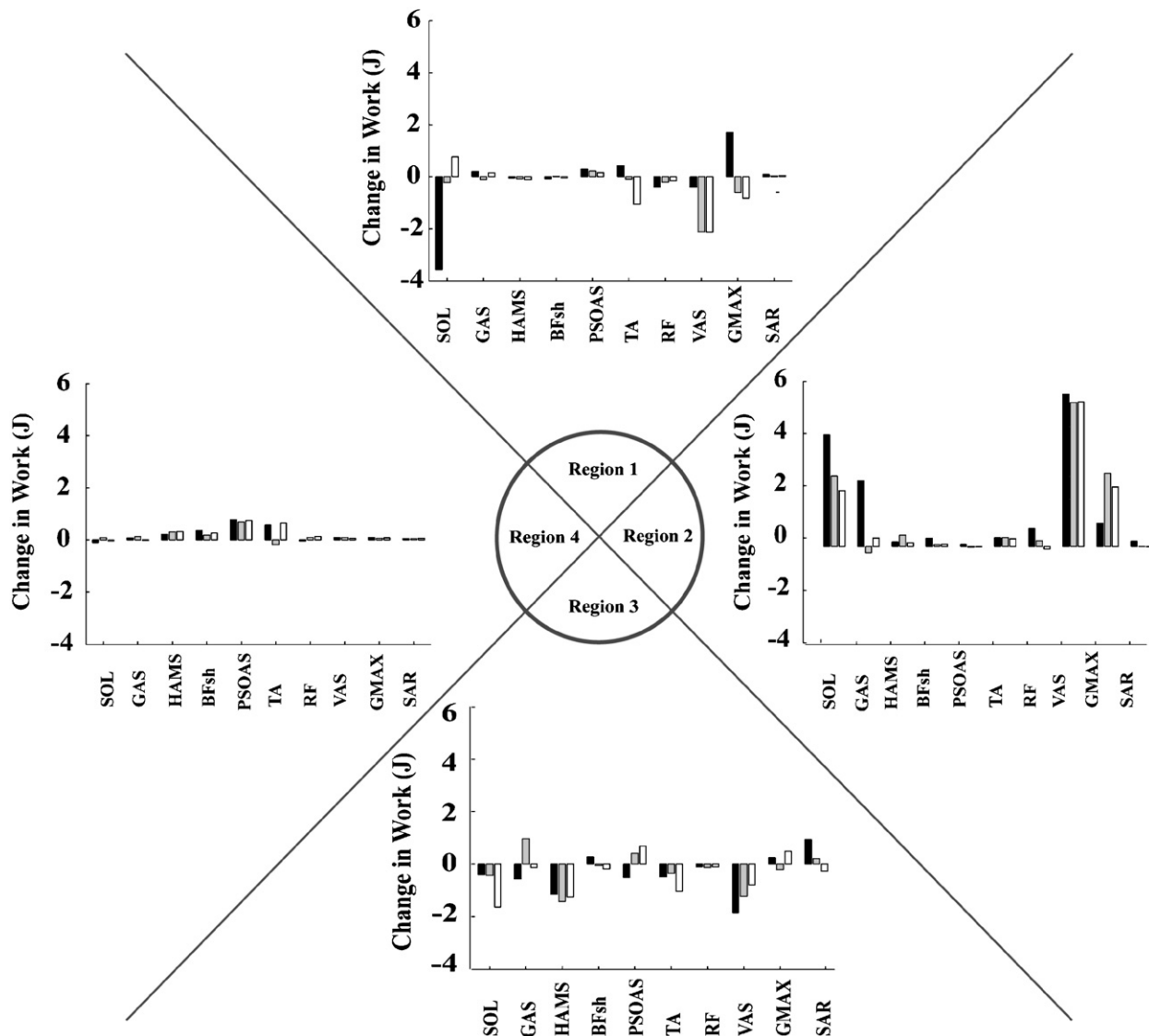
Fig. 5. Differences in single-leg muscle work within each region between the optimal and circular chainring shapes over one crank cycle. Black, gray and white bars represent differences at pedaling rates of 60, 90 and 120 rpm, respectively. Single-leg power output for all simulations ranged from 417.3 to 526.4 W.

phase. Kautz et al. (1994) measured increased crank power during regions of lower crank velocity produced by noncircular chainrings that were similar in shape to the present study. Miller and Ross (1980) developed a theoretical model of the crank torque developed by muscles as a function of crank angle and velocity and used optimization to identify the crank angular velocity profile that maximized average crank power. This also resulted in a velocity profile that slowed down the crank during the power phase to allow muscles to generate power for a longer duration. Similarly, Santalla et al. (2002) found a small improvement in delta efficiency (i.e., the ratio of the change in work accomplished to the change in energy expenditure) while using a crank mechanism that changed the relative angle between the pedals and allowed more time to be spent in the power phase. In addition to these pedaling studies,

Askew and Marsh (1997) provided a number of examples that suggest animals dramatically increase muscle power output during cyclical movements by prolonging the positive work phase. Thus, allowing muscles to generate power longer through an eccentric chainring is an effective mechanism to increase the average power output.

An interesting finding was that the optimal chainring shape and orientation for all three pedaling rates were similar, although there was a small systematic decrease in eccentricity as pedaling rate increased (Fig. 4). This systematic decrease in eccentricity was consistent with Neptune and Kautz (2001), who showed there is a trade-off between maximizing the time spent generating power during the downstroke and minimizing negative work that occurs during deactivation in the subsequent bottom transition phase (e.g., Fig. 5, Region 3). The optimal
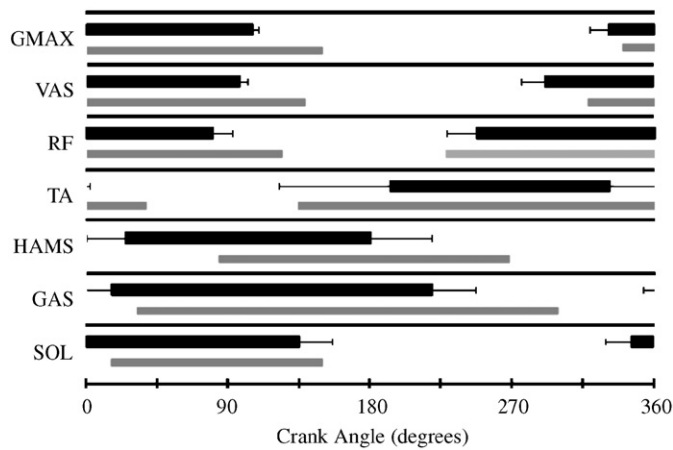
Fig. 6. Simulation muscle excitation timing for the circular chainring compared to experimental data at 90 rpm (taken from Neptune et al., 1997). Black bars indicate experimental data (±1 S.D.) during steady-state submaximal pedaling; gray bars indicate the solution obtained by the optimization. Comparable results were found for the other simulations with a systematic phase advance in timing observed for most muscle groups as the pedaling rate increased. Crank angle is defined as 0° at top-dead-center and positive in the clockwise direction.

eccentric chainring shape and orientation caused muscles to quickly change from shortening to lengthening as they were deactivating following the power phase (Fig. 2, Region 3), resulting in an increase in negative work that decreases the net power output. This is especially important at higher pedaling rates, where increases in negative crank work have been observed experimentally with conventional circular chainrings (Neptune and Herzog, 1999; Samozino et al., 2007).

To further assess the influence of activation–deactivation dynamics on chainring shape and power output, a sensitivity analysis on the time constants in the model was performed at 90 rpm. The analysis showed that faster time constants resulted in more eccentric chainring shapes as well as an increase in average crank power due primarily to a reduction in the amount of negative crank work produced following the power phase. Similarly, slower time constants decreased both the chainring eccentricity and average power output due to an increase in negative muscle work. These results were similar to Soest and Casius (2000) who showed the net crank power increased dramatically when activation–deactivation dynamics were removed from their model. This may explain why Hull et al. (1992) did not observe any differences in gross efficiency during submaximal pedaling at 90 rpm while analyzing an elliptical chainring with an eccentricity of 1.36, as the increased positive work output made possible by the chainring eccentricity may have been offset by increased negative work. These results suggest that it is important to consider an individual's muscle fiber composition when customizing chainring shapes to improve performance. For example, an endurance cyclist with predominantly more slow twitch fibers and consequently slower deactivation

dynamics may find greater improvements in power output with less eccentric shapes. Thus, the results of the present study could be further refined by developing subject-specific models that include activation–deactivation dynamics and force–velocity relationships based on fiber type (e.g., Umberger et al., 2006) to better match chainring shapes to individuals.

A potential concern with any non-circular chainring is the possibility of elevated joint loading due to increased crank accelerations and/or duration of high joint forces relative to those using a circular chainring. In order to investigate this possibility, a post hoc analysis was performed to compare the resulting joint loads between the optimal (eccentricity of 1.29) and circular chainrings at 90 rpm using the methods of Neptune and Kautz (2000). Of particular interest were the knee joint loads, which are a common mechanism for overuse injuries in cycling (e.g., Holmes et al., 1991; Weiss, 1985; Wilber et al., 1995). The analysis showed that there was little difference in average and peak knee joint forces between the two chainrings. However, during the power phase (Fig. 2, Region 2) when the largest intersegmental joint forces are produced, the increased duration produced by the optimal shape resulted in an average of 9.4% higher knee joint force impulses that may increase the potential for injury. On the other hand, the analysis also showed that within the region where the knee is most flexed (Fig. 2, Region 1), there was a greater than 45% reduction in both the shear and normal force impulses in the patellofemoral joint and the shear force impulse in the tibiofemoral joint while using the optimal chainring. This suggests the optimal chainring may provide a lower potential for knee injuries when the joint is most susceptible to injury (Neptune and Kautz, 2000).

Although our results are consistent with experimental observations, a potential limitation is that we used a hill-type muscle model that did not include history dependent effects such as force enhancement from stretch-shortening (e.g., Herzog and Leonard, 2000; Meijer et al., 1998), force depression following shortening contractions (e.g., Huijing, 1998; Lee et al., 2001) and changes in activation–deactivation dynamics during fast cyclical motions (e.g., Askew and Marsh, 1998; Brown and Loeb, 2000). However, the influence of these effects is dependent on the previous and current states of the muscle fibers (i.e., fiber length, velocity and activation), which were similar between the circular and non-circular chainrings (Fig. 7). Thus, the relative differences in power between chainrings would most likely remain the same. As these properties are further understood in whole body dynamic tasks (Herzog, 2004), the fidelity of the model can be improved and the influence of these effects on chainring shape can be assessed.

Another potential limitation is that we prescribed the crank angular velocity similar to that of an isokinetic ergometer, and therefore drive train dynamics were not included in the model. This was necessary within our model and optimization framework to assure the velocity profiles
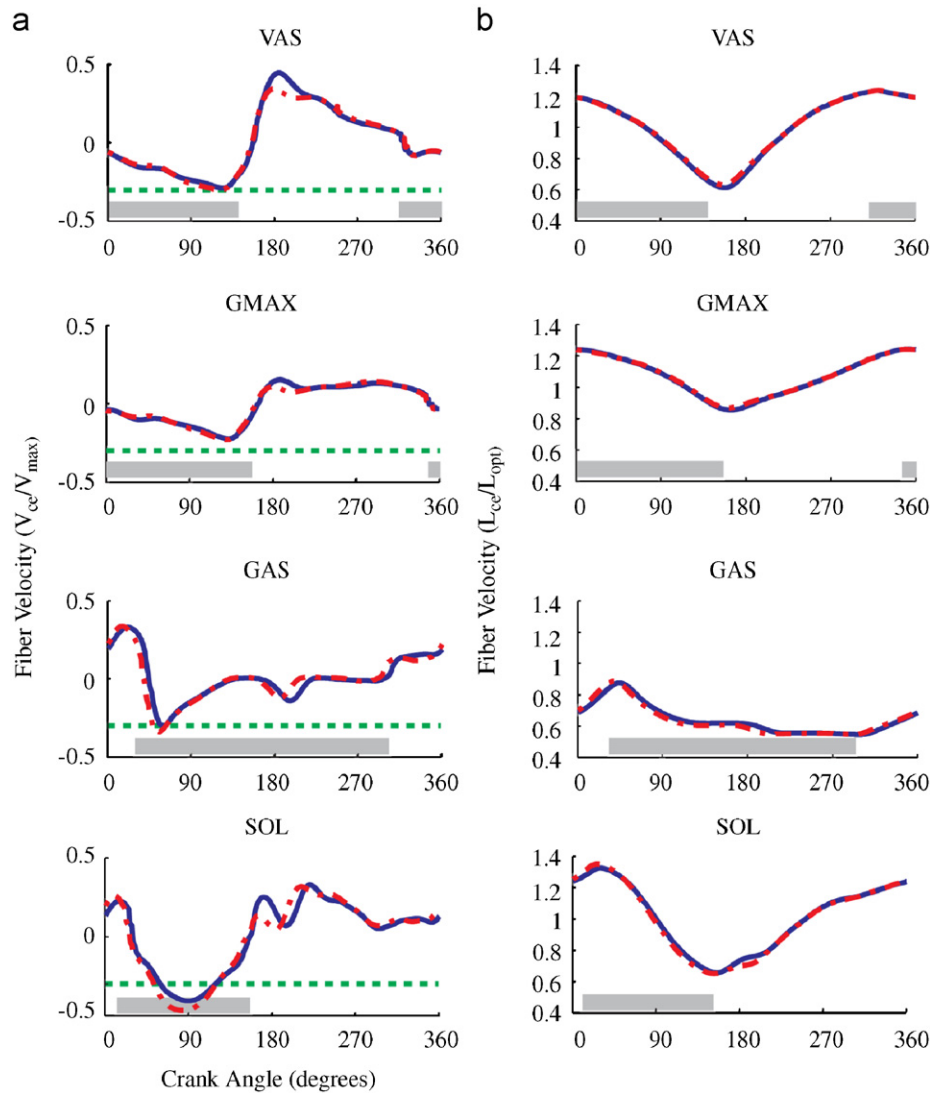
Fig. 7. Normalized muscle fiber states as a function of crank angle for the VAS, GMAX, GAS and SOL muscles at 90 rpm. (a) Fiber velocities (fiber shortening is negative, horizontal dotted line indicates the theoretical velocity at which maximal power is produced, 0.33 Vmax), and (b) fiber lengths. The thick gray bars indicate when the muscle is active. The dash-dot and solid lines represent the circular and optimal chainrings, respectively. The fiber length was normalized to its optimal length and the velocity was normalized to its maximum contraction velocity, which was estimated as ten times the muscle fiber resting length per second (Zajac, 1989).

of the optimal chainring shapes. However, previous studies have shown that the crank inertial load has little effect on pedaling coordination (Bertucci et al., 2005; Fregly et al., 1996) and Soest and Casius (2000) successfully reproduced experimental data while prescribing the motion of the crank with a similar pedaling model. Thus, the isokinetic nature of the present model would appear to have minimal influence on the optimal chainring shape.

A final potential limitation is that we fixed the hip motion in our model as this simplified the modeling and previous work has shown the fixed-hip assumption has minimal influence on hip joint power (Neptune and Hull, 1995). While imposing a known hip motion could have been done for the circular chainring, we could not have imposed a known motion for the non-circular chainring

since the corresponding motion was not known a priori. However, the motion would likely be similar between chainrings and have a similar effect on the muscle kinematics and corresponding muscle power. Thus, the relative difference in power output between chainrings would be similar. Further, the results showed that the mechanism for the increased power by the non-circular chainring was the increased power phase duration, not an alteration in the muscle kinematics. Thus, the fixed hip assumption would appear to have minimal impact on the optimal chainring shape and conclusions of the study.

While our study specifically investigated the ability of a non-circular chainring to improve cycling performance by increasing maximal power output during isokinetic

conditions, we believe that it is very likely that these results are also relevant to endurance pedaling during submaximal conditions. The pedaling pattern is very robust with muscle excitation timing being similar between maximal power pedaling and submaximal pedaling (Fig. 6). Thus, it is likely that the concept of allowing more time during the powerstroke and less time during transitions will be beneficial to both modes of cycling performance. Future theoretical analyses should seek to determine if similar benefits occur when using the optimal shape in endurance cycling.

Our study suggests that average crank power output can be increased by utilizing a non-circular chainring that allows muscles to generate power for a longer duration during the power phase (Fig. 2, Region 2). The results also showed that activation–deactivation dynamics is a key determinant of the optimal chainring's eccentricity. Although intersegmental joint load impulses increased during the power phase, the impulses were decreased by over 45% near top-dead-center when the knee is most susceptible to injury, suggesting that the optimal chainring may actually reduce the potential for knee injuries. Future work should be directed at experimentally validating the optimal chainring's ability to improve performance by analyzing both biomechanical and metabolic variables.

Conflict of interest statement

None .

Acknowledgments

The authors would like to thank Steve Kautz, Maury Hull and Wayne Stetina for their insightful discussions regarding optimal chainring shapes.

References

Askew, G.N., Marsh, R.L., 1997. The effects of length trajectory on the mechanical output of mouse skeletal muscles. Journal of Experimental Biology 200, 3119–3131.

Askew, G.N., Marsh, R.L., 1998. Optimal shortening velocity (V/V_{max}) of skeletal muscle during cyclical contractions: length–force effects and velocity-dependent activation and deactivation. Journal of Experimental Biology 201, 1527–1540.

Bertucci, W., Grappe, F., Girard, A., Betik, A., Rouillon, J.D., 2005. Effects on the crank torque profile when changing pedalling cadence in level ground and uphill road cycling. Journal of Biomechanics 38, 1003–1010.

Brown, I.E., Loeb, G.E., 2000. Measured and modeled properties of mammalian skeletal muscle: IV. dynamics of activation and deactivation. Journal of Muscle Research and Cell Motility 21, 33–47.

Cullen, L.K., Andrew, K., Lair, K.R., Widger, M.J., Timson, B.F., 1992. Efficiency of trained cyclists using circular and noncircular chainrings. International Journal of Sports Medicine 13, 264–269.

Davy, D.T., Audu, M.L., 1987. A dynamic optimization technique for predicting muscle forces in the swing phase of gait. Journal of Biomechanics 20, 187–201.

Durfee, W.K., Palmer, K.I., 1994. Estimation of force–activation, force–length, and force–velocity properties in isolated, electrically stimulated muscle. IEEE Transactions on Biomedical Engineering 41, 205–216.

Fregly, B.J., Zajac, F.E., Dairaghi, C.A., 1996. Crank inertial load has little effect on steady-state pedaling coordination. Journal of Biomechanics 29, 1559–1567.

Goffe, W.L., Ferrier, G.D., Rogers, J., 1994. Global optimization of statistical functions with simulated annealing. Journal of Econometrics 60, 65–99.

Hagberg, J.M., Mullin, J.P., Giese, M.D., Spitznagel, E., 1981. Effect of pedaling rate on submaximal exercise responses of competitive cyclists. Journal of Applied Physiology 51, 447–451.

Herzog, W., 2004. History dependence of skeletal muscle force production: implications for movement control. Human Movement Science 23, 591–604.

Herzog, W., Leonard, T.R., 2000. The history dependence of force production in mammalian skeletal muscle following stretch-shortening and shortening-stretch cycles. Journal of Biomechanics 33, 531–542.

Holmes, J.C., Pruitt, A.L., Whalen, N.J., 1991. Cycling knee injuries. Cycling Science 3, 11–14.

Hue, O., Galy, O., Hertogh, C., Casties, J.F., Prefaut, C., 2001. Enhancing cycling performance using an eccentric chainring. Medicine and Science in Sports and Exercise 33, 1006–1010.

Huijing, P.A., 1998. Muscle, the motor of movement: properties in function, experiment and modelling. Journal of Electromyography and Kinesiology 8, 61–77.

Hull, M.L., Williams, M., Williams, K., Kautz, S., 1992. Physiological response to cycling with both circular and noncircular chainrings. Medicine and Science in Sports and Exercise 24, 1114–1122.

Kautz, S.A., Hull, M.L., 1995. Dynamic optimization analysis for equipment setup problems in endurance cycling. Journal of Biomechanics 28, 1391–1401.

Kautz, S.A., Hull, M.L., Neptune, R.R., 1994. A comparison of muscular mechanical energy expenditure and internal work in cycling. Journal of Biomechanics 27, 1459–1467.

Lee, H.D., Herzog, W., Leonard, T., 2001. Effects of cyclic changes in muscle length on force production in in-situ cat soleus. Journal of Biomechanics 34, 979–987.

Lucia, A., Balmer, J., Davison, R.C., Perez, M., Santalla, A., Smith, P.M., 2004. Effects of the rotor pedalling system on the performance of trained cyclists during incremental and constant-load cycle-ergometer tests. International Journal of Sports Medicine 25, 479–485.

Marsh, A.P., Martin, P.E., 1993. The association between cycling experience and preferred and most economical cadences. Medicine and Science in Sports and Exercise 25, 1269–1274.

Martin, J.C., Lamb, S.M., Brown, N.A., 2002. Pedal trajectory alters maximal single-leg cycling power. Medicine and Science in Sports and Exercise 34, 1332–1336.

Martinez, A.C., Vicente, G.V., Calvo, J.S., Zudaire, I.L., 2006. Preliminary Report on Q-Rings. University of Vallodolid, Spain.

Meijer, K., Grootenboer, H.J., Koopman, H.F., van der Linden, B.J., Huijing, P.A., 1998. A hill-type model of rat medial gastrocnemius muscle that accounts for shortening history effects. Journal of Biomechanics 31, 555–563.

Miller, N.R., Ross, D., 1980. The design of variable ratio chain drives for bicycles and ergometers—application to maximum power bicycle drive. Journal of Mechanical Design 102, 711–717.

Neptune, R.R., Hull, M.L., 1995. Accuracy assessment of methods for determining hip movement in seated cycling. Journal of Biomechanics 28, 423–437.

Neptune, R.R., Herzog, W., 1999. The association between negative muscle work and pedaling rate. Journal of Biomechanics 32, 1021–1026.

Neptune, R.R., Kautz, S.A., 2000. Knee joint loading in forward versus backward pedaling: implications for rehabilitation strategies. Clinical Biomechanics 15, 528–535.

Neptune, R.R., Kautz, S.A., 2001. Muscle activation and deactivation dynamics: the governing properties in fast cyclical human movement performance? Exercise and Sport Science Reviews 29, 76–80.

Neptune, R.R., Kautz, S.A., Hull, M.L., 1997. The effect of pedaling rate on coordination in cycling. Journal of Biomechanics 30, 1051–1058.

Okajima, S., 1983. Designing chainwheels to optimize the human engine. Bike Techniques 2, 1–7.

Raasch, C.C., Zajac, F.E., Ma, B., Levine, W.S., 1997. Muscle coordination of maximum-speed pedaling. Journal of Biomechanics 30, 595–602.

Ratel, S., Duche, P., Hautier, C.A., Williams, C.A., Bedu, M., 2004. Physiological responses during cycling with noncircular "harmonic" and circular chainrings. European Journal of Applied Physiology 91, 100–104.

Samozino, P., Horvais, N., Hintzy, F., 2007. Why does power output decrease at high pedaling rates during sprint cycling? Medicine and Science in Sports and Exercise, 680–687.

Santalla, A., Manzano, J.M., Perez, M., Lucia, A., 2002. A new pedaling design: the rotor effects on cycling performance. Medicine and Science in Sports and Exercise 34, 1854–1858.

Sargeant, A.J., 1994. Human power output and muscle fatigue. International Journal of Sports Medicine 15, 116–121.

Soest, A.J., Casius, L.J.R., 2000. Which factors determine the optimal pedal rate in cycling? Medicine and Science in Sports and Exercise 32, 1927–1934.

Umberger, B.R., Gerritsen, K.G., Martin, P.E., 2006. Muscle fiber type effects on energetically optimal cadences in cycling. Journal of Biomechanics 39, 1472–1479.

Weiss, B.D., 1985. Nontraumatic injuries in amateur long distance bicyclists. American Journal of Sports Medicine 13, 187–192.

Wilber, C.A., Holland, G.J., Madison, R.E., Loy, S.F., 1995. An epidemiological analysis of overuse injuries among recreational cyclists. International Journal of Sports Medicine 16, 201–206.

Yamaguchi, G.T., Zajac, F.E., 1989. A planar model of the knee joint to characterize the knee extensor mechanism. Journal of Biomechanics 22, 1–10.

Zajac, F.E., 1989. Muscle and tendon: properties, models, scaling, and application to biomechanics and motor control. Critical Reviews in Biomedical Engineering 17, 359–411.

Zamparo, P., Minetti, A., di Prampero, P., 2002. Mechanical efficiency of cycling with a new developed pedal-crank. Journal of Biomechanics 35, 1387–1398.